AD-A033 830 COLD REGIONS RESEARCH AND ENGINEERING LAB HANOVER N H F/G 20/13
THERMODYNAMIC DEFORMATION OF WET SNOW,(U)
NOV 76 S C COLBECK

UNCLASSIFIED CRREL-76-44 NL

| OF |
AD
A033830

END

DATE
FILMED
2-77

CRREL
REPORT 76-44

Thermodynamic deformation of wet snow

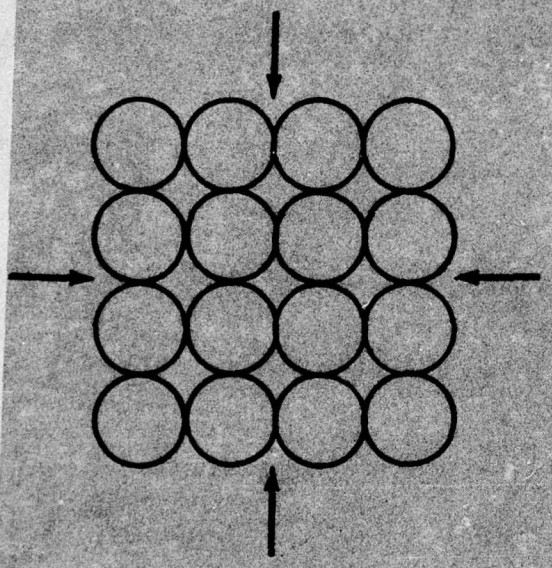

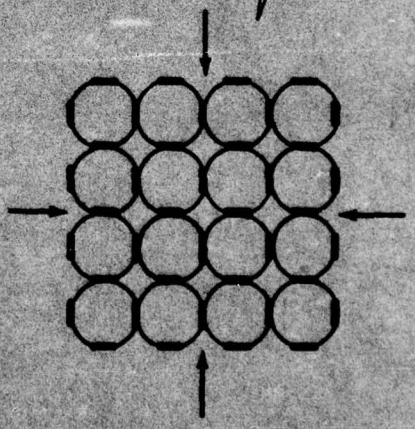

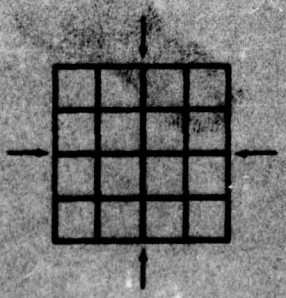

For conversion of SI metric units to U.S./British customary units of measurement consult ASTM Standard E380, Metric Practice Guide, *published by the American Society for Testing and Materials, 1916 Race St., Philadelphia, Pa. 19103.*

Cover: Compression by contact melting.

CRREL Report 76-44

Thermodynamic deformation of wet snow

Samuel C. Colbeck

November 1976

Prepared for
DIRECTORATE OF MILITARY CONSTRUCTION
OFFICE, CHIEF OF ENGINEERS
By
CORPS OF ENGINEERS, U.S. ARMY
COLD REGIONS RESEARCH AND ENGINEERING LABORATORY
HANOVER, NEW HAMPSHIRE

Unclassified

SECURITY CLASSIFICATION OF THIS PAGE (When Data Entered)

REPORT DOCUMENTATION PAGE		READ INSTRUCTIONS BEFORE COMPLETING FORM
1. REPORT NUMBER (14) CRREL ~~Report~~ 76-44	2. GOVT ACCESSION NO.	3. RECIPIENT'S CATALOG NUMBER
4. TITLE (and Subtitle) (6) THERMODYNAMIC DEFORMATION OF WET SNOW (9)		5. TYPE OF REPORT & PERIOD COVERED
		6. PERFORMING ORG. REPORT NUMBER
7. AUTHOR(s) (10) Samuel C. Colbeck		8. CONTRACT OR GRANT NUMBER(s)
9. PERFORMING ORGANIZATION NAME AND ADDRESS U.S. Army Cold Regions Research and Engineering Laboratory Hanover, New Hampshire		10. PROGRAM ELEMENT, PROJECT, TASK AREA & WORK UNIT NUMBERS DA Proj. 4A161102AT24, Task A03, E01 Work Unit 001 and DA Proj. 1T161102 B52A Task 02, Work Unit 003
11. CONTROLLING OFFICE NAME AND ADDRESS Directorate of Military Construction Office, Chief of Engineers Washington, D.C.		12. (11) REPORT DATE November 1976
		13. NUMBER OF PAGES 13 (12) 16 pp.
14. MONITORING AGENCY NAME & ADDRESS (if different from Controlling Office)		15. SECURITY CLASS. (of this report) Unclassified
		15a. DECLASSIFICATION/DOWNGRADING SCHEDULE

16. DISTRIBUTION STATEMENT (of this Report)

(16) 4A161102AT24, 1T161102B52A

Approved for public release; distribution unlimited.

(17) 03, 02

17. DISTRIBUTION STATEMENT (of the abstract entered in Block 20, if different from Report)

18. SUPPLEMENTARY NOTES

19. KEY WORDS (Continue on reverse side if necessary and identify by block number)

Deformation
Rheology
Snow
Thermodynamics

20. ABSTRACT (Continue on reverse side if necessary and identify by block number)

The deformation of wet snow is explained in terms of the thermodynamics of the three phases of water. When deformation by particle rearrangement is fully developed, deformation can occur most rapidly by melting at the particle contacts. The rate of deformation is highly sensitive to the liquid water content, ionic impurity content, particle contact area, and stress level. A model of the hydrostatic deformation of wet snow is constructed, and examples of the deformation of wet snow are given for a variety of conditions. These results are in agreement with existing experimental evidence. The model accurately simulates the transient nature of the deformation and the effect of water content on the quasi-stable density of wet snow subjected to a constant stress.

037 100

DD FORM 1 JAN 73 1473 EDITION OF 1 NOV 65 IS OBSOLETE

Unclassified

SECURITY CLASSIFICATION OF THIS PAGE (When Data Entered)

6pg

PREFACE

This report was prepared by Dr. Samuel C. Colbeck, Geophysicist, of the Snow and Ice Branch, Research Division, U.S. Army Cold Regions Research and Engineering Laboratory. The research was funded by DA Project 4A161102AT24, *Research in Snow, Ice, and Frozen Ground*, Scientific Area 03, *Research in Terrain and Climatic Constants*, Scientific Effort 01, *Cold Environment Factors*, Work Unit 001, *Research in Snow Mechanics*, and by DA Project 1T161102B52A, *Mobility and Environmental Research*, Task 02, *Military Aspects of Cold Regions Research*, Work Unit 003, *Research in Snow Mechanics* (QCR CARDS 111a, 110b).

Dr. Malcolm Mellor, Dr. William Harrison, and Nancy Parssinen of CRREL technically reviewed the manuscript.

LIST OF SYMBOLS

d	thickness of water film
D	depth (or displacement) of melted cap
F	force between particles
k	thermal conductivity of ice
L	latent heat of fusion
n_s	moles of solute
n_w	moles of water
p	pressure in the liquid phase
p_0	pressure in the liquid at the center of the contact
P_b	pressure at the bond
P_c	capillary pressure
q	water flux in film
Q	heat flux
r	polar coordinate
r_a	radius of air bubble
r_b	radius of contact
r_0	initial particle radius
r_p	particle radius
R	gas constant for water vapor
T_b	temperature of bond
T_0	273 K
T_s	temperature of curved particle surface
μ	viscosity of water
ρ	density of snow sample considering ice phase only
ρ_ℓ	liquid water density
ρ_0	initial ice density of snow sample
ρ_s	density of ice
$\sigma_{\ell g}$	liquid/vapor interfacial tension
σ_{sg}	solid/gas interfacial tension
$\sigma_{s\ell}$	solid/liquid interfacial tension

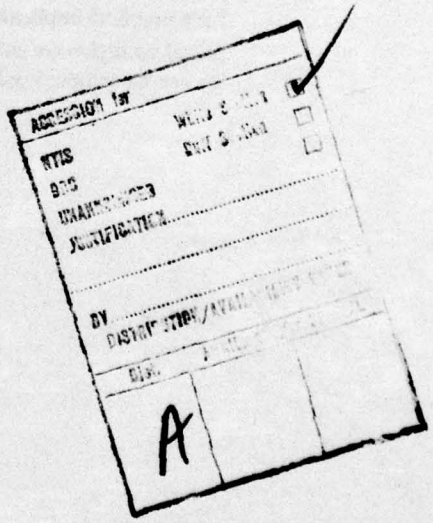

SUMMARY

The rheology of wet snow controls over-snow movement in the cold regions during much of the year. The deformation of wet snow is equally important to traffic movement over highways and to the release of wet snow avalanches. The thermodynamics of wet snow controls its rapid deformation in a manner unlike the deformation of dry snow. Because of the presence of liquid water, wet snow can deform rapidly by melting at the inter-particle contacts and refreezing at the curved ice surfaces. The rate of deformation is controlled by the parameters which determine the temperature difference between the inter-particle contacts and the curved ice surfaces. The temperature of the contact is determined strictly by the force between the particles and the size of the contact. The temperature of the curved surface is determined by the particle size, ionic impurity content of the liquid phase, and air bubble size or capillary pressure. As the inter-particle bond size increases, the inter-particle stress decreases and the bond temperature increases until the temperature differences around a particle are equalized. At that time the rapid thermodynamic deformation described here ceases, and further deformation must proceed by more efficient packing arrangements and/or the normal processes of crystalline deformation.

Using a simple geometrical packing arrangement (see cover of this report) and the principles of thermodynamics, a simple model of wet snow deformation is constructed here. The results of this model are qualitatively similar to the experimental results, including a lower value of maximum density at larger values of capillary pressures. The effect of ionic impurities on the maximum bond size is also calculated and found to be the same as increasing the capillary pressure. The hardening effects of increasing capillary pressure and/or ionic impurity content have practical implications. For example, the optimum use of salt for snow removal on highways and for hardening wet snow for increased over-snow mobility can be achieved only through the understanding of wet snow rheology.

THERMODYNAMIC DEFORMATION OF WET SNOW

Samuel C. Colbeck

INTRODUCTION

The rheology of snow at subfreezing temperatures has been extensively researched and much useful information has been generated (see Mellor 1975). Unfortunately, the rheology of snow which contains liquid water has been almost totally ignored. This disparity does not arise because wet snow is any less important than snow at lower temperatures – witness the destructive powers of wet snow slides and the highway hazards caused by the compaction of wet snow into ice. It probably arises from the greater difficulties of handling wet snow samples and of understanding the complex interaction between the thermodynamic and mechanical aspects of wet snow deformation.

For a given stress, the deformation of wet snow generally occurs much more rapidly than can be explained by intracrystalline straining and/or more efficient grain packing; hence, some thermodynamic explanation must be invoked. Colbeck (1973) described some of the important aspects of the phase thermodynamics of wet snow. The equilibrium temperature among the three phases of water in wet snow is controlled by the size of the spherical grains, water content, grain contact area, impurity content, porosity, and stress. The thermodynamic and geometric principles which relate the deformation to these variables are used here to describe the densification of wet snow at high strain rates. The slow deformation of wet snow in situations where intracrystalline creep or grain repacking are the dominant mechanisms is not considered here.

THERMODYNAMICS

The thermodynamic deformation of wet snow is controlled by the temperature difference between the inter-particle contacts and the ice/fluid interfaces

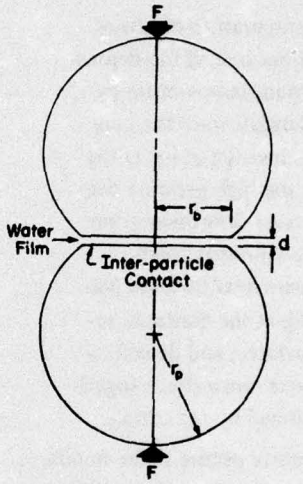

Figure 1. Schematic representation of two particles moving together by melting at their mutual contact. The size of the particle r_p, size of the bond r_b, and thickness of the water film d are shown.

(Fig. 1). The temperature at a contact is determined exclusively by its area and the average normal force acting across it. During rapid deformation no shear forces can be supported by an inter-particle contact because the ice surfaces are separated by a water film of sufficient thickness to prevent ice-to-ice contact. The thickness of this film, as determined by the rate of deformation, is described below.

The temperature of the free surface away from the inter-particle contact is determined by the radius of the particles, radius of the air/liquid interface, and impurity content of the liquid phase in the pores. Depending on the direction of heat flow, there are three possible mechanical states.

1. When the surface temperature T_s is less than the contact temperature T_b, heat flows away from the contact and produces freezing in the liquid layer. Thus the inter-particle strength tends to increase. This regime occurs when the snow is frozen either by spreading salt on a wet snow surface or by withdrawing the liquid. Accordingly, the relatively rapid

thermodynamic deformation ceases and the wet snow deforms by the same mechanisms as dry snow. If a higher stress or more liquid is introduced, the contacts may melt again.

2. When the pore surface and contact temperatures are equal, no heat flow occurs, but a significant inter-particle strength can develop slowly due to ice-to-ice adhesion. The liquid tension may cause some additional inter-particle strength (Moore and Millar 1971, Skelton 1975).

3. When the lowest temperature occurs at the inter-particle contact because of the depression of the phase equilibrium temperature by the contact stress, heat flows toward the contact causing a continuous melting of ice at the contact. This melting at the high pressure contact is accompanied by water flow away from the contact toward the low pressure pore water. Thus water flow and heat flow are balanced, resulting in melting at the contacts, refreezing on the curved surfaces, and densification as the particle contacts move closer together and the porosity is reduced by refreezing.

When the lowest temperature occurs at the bonds, rapid densification can occur even at moderate levels of normal stress transmitted across the contacts. The contact temperature during rapid densification is independent of impurities in the pore water because meltwater moves away from the contact. Accordingly, the equilibrium temperature T_b for the nearly flat contact surface is given by*

$$T_b = \frac{P_b T_0}{L}\left(\frac{1}{\rho_\ell} - \frac{1}{\rho_s}\right) \qquad (1)$$

where P_b = pressure of the bond
T_0 = 273 K
L = latent heat of fusion
ρ_ℓ = liquid water density
ρ_s = density of ice.

The phase-equilibrium temperature on the rounded particle surface depends upon the saturation regime of the wet snow (Colbeck 1973). The equilibrium temperature in the funicular regime of high liquid saturation is determined by the ice particle radius r_p and air bubble radius r_a according to

$$T_s = \frac{2T_0}{L}\left(\frac{1}{\rho_\ell} - \frac{1}{\rho_s}\right)\frac{\sigma_{\ell g}}{r_a} - \frac{2T_0}{L\rho_s}\frac{\sigma_{s\ell}}{r_p} - \frac{RT_0^2}{L}\frac{n_s}{n_w} \qquad (2)$$

where $\sigma_{\ell g}$ = liquid/vapor interfacial tension
$\sigma_{s\ell}$ = solid/liquid interfacial tension
R = gas content in water vapor
n_s/n_w = temperature depression caused by the presence of ionic impurities.

Similarly, the equilibrium in the pendular regime of low saturations is determined by the particle size, ionic impurity content, and capillary pressure P_c according to

$$T_s = -\frac{T_0}{\rho_\ell L}P_c - \frac{2T_0}{L\rho_s}\frac{\sigma_{sg}}{r_p} - \frac{RT_0^2}{L}\frac{n_s}{n_w} \qquad (3)$$

where σ_{sg} is the solid/gas interfacial tension.

Ionic impurities, capillary pressures and small particle sizes reduce the temperature of the curved particle surface; the heat flow to the bonds is reduced accordingly. The rate of deformation, ultimate bond size, and maximum density achievable by rapid thermodynamic densification are also reduced. In snow which is unstressed but saturated, particle size increases rapidly to the quasi-stable diameter of 1 to 3 mm (Wakahama 1968, Colbeck 1973). At this time the effect of particle size on the phase equilibrium temperature is only 10^{-5} to 10^{-4} °C, or about the same as the effect of impurities in natural snow.

Capillary pressure increases as water saturation decreases, as shown experimentally by Colbeck (1973). Thus, at high water saturations where P_c is small, the curved surface temperature is high; therefore, heat flow into the inter-particle contact and rapid densification are more likely. As water saturation is reduced and capillary pressure increases, the rate of densification is reduced accordingly. The experimental results of Tusima (1973) and Kinosita (1963) demonstrate this fact. In principle the effect of an increase in capillary pressure could be as large as -0.01°C and profoundly influence the response of wet snow to stress. In practice, however, this effect is greatly reduced by the time required to achieve large capillary pressures in large grained materials.

** The effect of dissolved air has been neglected because of uncertainty about the air content of the meltwater at the contacts.*

Harris and Morrow (1964) showed that reduction of liquid pressure is delayed during drainage because of the slow process of liquid movement through thin films on particle surfaces. Their results suggest that Colbeck's (1973) capillary pressure-water saturation curve does not quite represent true capillary equilibrium, because the experiment was completed too quickly to allow complete drainage at each pressure level. Thus, while capillary pressure can have a large effect on the densification of wet snow, many days may be required for complete liquid drainage from wet snow subjected to large capillary pressures. Much experimental work remains to be done on the capillary equilibrium in the pendular regime of saturation to determine the circumstances necessary for achieving large capillary pressures in wet snow samples. The main experimental problem is the loss of liquid contact between the sample and the porous plate through which the liquid is extracted. Occasionally it is possible to measure large capillary pressures in wet snow (Colbeck 1976), suggesting that loss of contact cannot necessarily be predicted in advance. This problem, which is common for porous materials with large grains, does not preclude the application of this theory of thermodynamic densification to samples subjected to large capillary pressures. However, it must be recognized that large capillary pressures are difficult to obtain experimentally.

HEAT AND MASS FLOW

When a lower temperature occurs at the inter-particle contact than at the particle surface, the heat flux Q approaching the contact can be determined by

$$Q = k \frac{T_s - T_b}{r_b} \tag{4}$$

where k is the thermal conductivity of ice and r_b the radius of the inter-particle bond. The contact melts at a rate given by

$$\frac{dD}{dt} = \frac{k}{L\rho_s} \frac{T_s - T_b}{r_b} \tag{5}$$

where D is the depth of the melted cap (see Fig. 2). Equation 5 gives the rate of approach of particle centers, but the particle size, impurity level, water content, and contact radius must be known to use this result. It is unlikely that the contact radius can be determined directly at any time for any given sample, although most of the other parameters can be measured. Accordingly, it is necessary either to know the complete history of a sample of wet snow or to relate the contact size to density through assumptions about the geometry of particle arrangements. The latter is done in the next section, *Particle Geometry*.

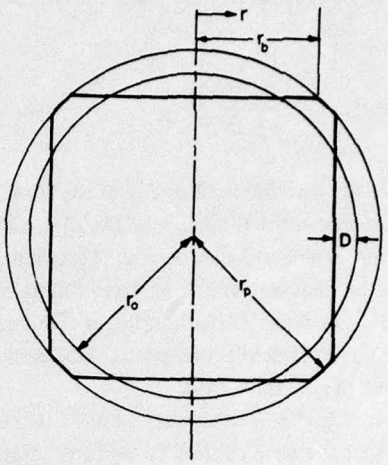

Figure 2. Cross-sectional view through the center of a sphere, showing the initial radius r_0, contact displacement D, contact radius r_b, and current particle radius r_p.

Assuming a constant thickness for the water film at the contact, heat and water flow must balance. At normal rates of densification, the thickness of the water film at the contact is apparently many times greater than an adsorbed layer of structured water. Therefore, the flux of water through the film q is described by

$$q = \frac{d^3}{12\mu} \frac{\partial p}{\partial r} \tag{6}$$

where d = thickness of the water film
p = pressure in the liquid phase
μ = viscosity of water
r = the radial coordinate.

By continuity, the flux of water increases with radius along the contact as

$$q = \frac{\rho_s}{\rho_\ell} \frac{dD}{dt} \frac{r}{d} . \tag{7}$$

Hence, for flat contacts, the pressure distribution along the water film,

$$p = p_0 - \frac{6\mu}{d^4}\,\frac{\rho_s}{\rho_\ell}\,\frac{dD}{dt}\,r^2 \qquad (8)$$

is very sensitive to the thickness d of the film. For small increases in the thickness of the film, a large change in pressure and flux occurs. Therefore, the film size must be relatively stable for large fluctuations in heat and water flow. Unfortunately q and d cannot be identified independently without making some assumption about the pressure field.

Although that is unnecessary here, it is important to note that pressure cannot be uniform along the inter-particle contact. A pressure drop toward the outside of the contact is necessary for water flow out of the contact and into the pore space. The parabolic distribution given by eq 8 shows a fairly uniform liquid pressure over most of the contact, with a rapid pressure drop near the edge of the contact. Thus the water film is capable of supporting the force between the particles with a maximum pressure p_0 only slightly higher than the average contact stress $F\pi^{-1} r_b^{-2}$. It is now apparent that the tension of the pore liquid affects both the phase equilibrium temperature of the pore space and the liquid pressure distribution in the contact. The first effect is manifested by a change in temperature distribution and rate of densification, while the second influences only the thickness of the liquid layer at the contact.

PARTICLE GEOMETRY

The rate at which the particle centers move closer together by contact melting can be calculated with eq 5, but it is necessary to specify the packing geometry to construct a model of wet snow densification (see cover of this report). Visscher and Bolsterli (1972) found an average of 6.4 contacts per sphere in random packings of uniform spheres, which is closely approximated by geometrically regular, cubic packing. A cubic model considerably simplifies the complicated geometry of a random packing, but does not adequately represent densification at porosities greater than 0.476. Higher porosities, which would have a lesser number of contacts, may be represented by allowing the number of contacts to increase to six as the 0.476 porosity is approached; however, some experimental testing of this approach must be made prior to its adoption.

Starting with a cubic packing of equal spheres, densification proceeds by melting at inter-particle contacts and refreezing in the pore spaces. The mass of each particle is constant, and we assume that each particle remains spherical, except for its six contact surfaces. At any time during densification, the depth of the melted cap D (see Fig. 2) is

$$D = r_0 - (r_p^2 - r_b^2)^{1/2} \qquad (9)$$

and the dry bulk density ρ of the sample is

$$\rho = \rho_0 \left(\frac{r_0}{r_0 - D}\right)^3 . \qquad (10)$$

The intersection of the spheres causes some error in these equations at higher densities, but this error is less than 1%. The increase in particle radius associated with the refreezing in the pore space is 14% of the cubic model's initial radius, and it must be accounted for in the model.

Since mass is conserved for each particle, the particle and contact radii are related to the initial radius by

$$r_0^3 = 4r_p^3 - 3(r_p^2 - r_b^2)^{3/2} - 4.5r_b^2(r_p^2 - r_b^2)^{1/2} . \qquad (11)$$

In principle it is now possible to solve for density as a function of time for any given set of conditions. However, algebraic problems make this approach impractical, and an iterative calculation of the deformation starting from the cubic packing of equal spheres is used instead. As an example of the geometrical relationships and as an aid in the iterative calculation, D and r_b are shown as functions of r_p in Figure 3.

Results derived from the model

As an example of the application of these concepts, the hydrostatic compression of saturated snow at a hydrostatic stress of 10^4 N m^{-2} * is calculated. Calculated values at steps in the iterative procedure are given in Table I and the results are shown on Figure 4. The depth of the melt cap D increases rapidly at first, because of the high stress concentration at the points of the spherical particles, but the rate of growth

* *1 N m^{-2} = 1 Pa.*

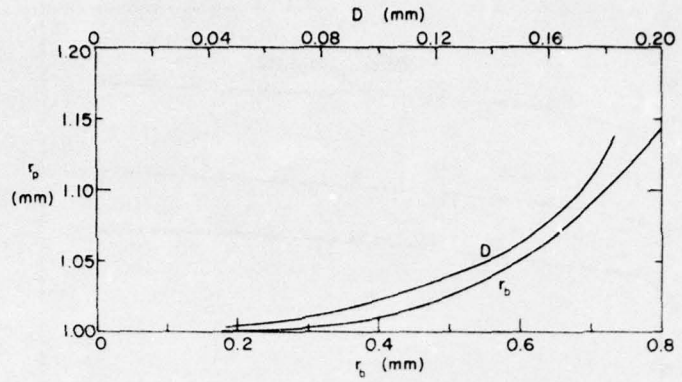

Figure 3. Depth of melted cap D *and bond radius* r_b *shown as a function of particle radius* r_p *for a particle with an initial radius* r_0 *of 1 mm.*

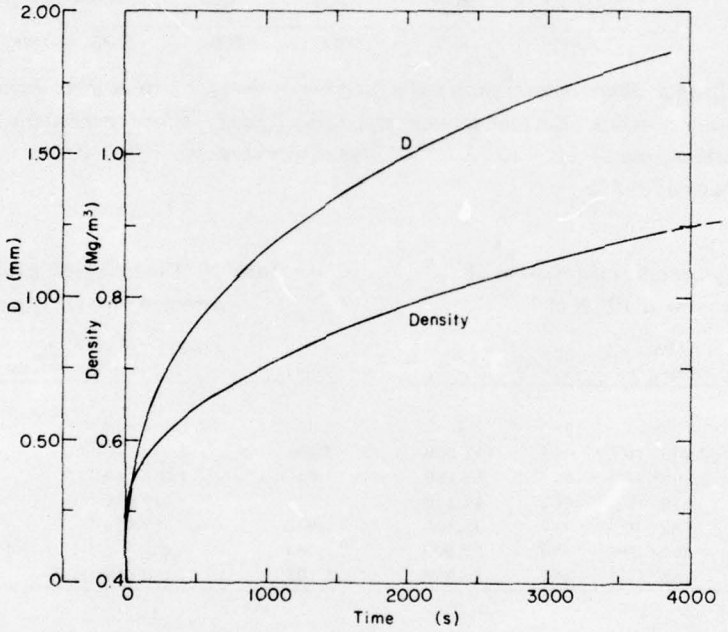

Figure 4. The ice density and depth of the melted cap D *shown as functions of time for a saturated sample compressed hydrostatically with a stress of* 10^4 *N* m^{-2}.

of the cap decreases as the cap volume increases. Likewise, the rate of density increase is a steadily decreasing function of time which approaches the density of solid ice asymptotically. Qualitatively these results are very similar to those of Tusima (1973), although his tests were done with repeated loadings at a stress of 3.25×10^5 N m^{-2} and showed a much more rapid response (see Fig. 5).

The rate of density increase is a complicated function of stress because of the complex relationships among the thermodynamic and geometrical variables which control the rate of density increase. However, as shown in Table II, the rate of growth of the melt cap increases approximately linearly with the increase in stress. Therefore the rate of increase in density,

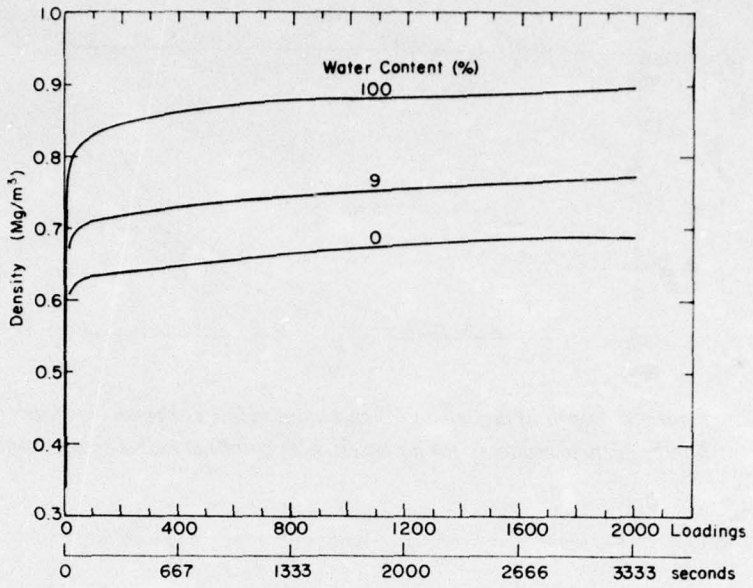

Figure 5. Snow density shown as a function of time for tests at three liquid water contents. The samples were repeatedly loaded (36 loads per minute) with a stress of 3.25×10^5 N m^{-2}. These curves were drawn from data in Tusima (1973).

Table I. The hydrostatic compression of saturated snow at 10^4 N m^{-2}.

r_p (mm)	r_b (mm)	D (mm)	dD/dt (mm s^{-1})	ρ (kg m^{-3})	P_b (N m^{-2})
1.0	0.	0	0	480	0
1.003	0.295	0.0413	$2{,}078 \times 10^{-7}$	445	112,000
1.01	0.4	0.072	$1{,}060 \times 10^{-7}$	602	68,100
1.022	0.487	0.101	618×10^{-7}	662	44,800
1.038	0.589	0.125	383×10^{-7}	718	31,100
1.062	0.634	0.149	262×10^{-7}	780	22,800
1.105	0.731	0.172	168×10^{-7}	845	16,050

Table II. The hydrostatic compression of saturated snow at two stresses.

(mm)	dD/dt (10^4 N m^{-2}) (mm s^{-1})	dD/dt (10^6 N m^{-2}) (mm s^{-1})
1.0	∞	∞
1.003	$2{,}078 \times 10^{-7}$	$2{,}100 \times 10^{-5}$
1.01	$1{,}060 \times 10^{-7}$	$1{,}070 \times 10^{-5}$
1.022	618×10^{-7}	622×10^{-5}
1.038	383×10^{-7}	391×10^{-5}
1.062	262×10^{-7}	268×10^{-5}
1.105	168×10^{-7}	173×10^{-5}

$$\frac{d\rho}{dt} = \frac{3\rho_0 r_0^3}{(r_0 - D)^4} \frac{dD}{dt} \qquad (12)$$

is approximately linearly related to stress when the load is first applied, but is a nonlinear function of stress at larger values of time because the denominator of eq 12 decreases with increasing deformation.

The decrease in phase equilibrium temperature associated with increasing capillary pressure reduces the heat flow from the particle surface to the inter-particle bond, as described previously. Thus, at lower liquid saturations, the thermodynamic deformation of wet snow proceeds more slowly, as shown by Tusima's (1973) results in Figure 5. Tusima's data suggest that the maximum density approaches a lower limit at lower water saturations, an expected result of lowering the phase equilibrium temperature on the particle's curved surface. As a further example of the effect of capillary pressure on the rate of deformation of wet snow, the calculated densities are shown as functions of time at a hydrostatic stress of 10^4 N m^{-2} and capillary pressures of 0, 0.1, 0.5 and 1 m of water (0, 987, 4935 and 9870 N m^{-2}) in Figure 6 and Table III. Although the stress levels were higher in Tusima's experiments where the stress was applied intermittently, Tusima's results

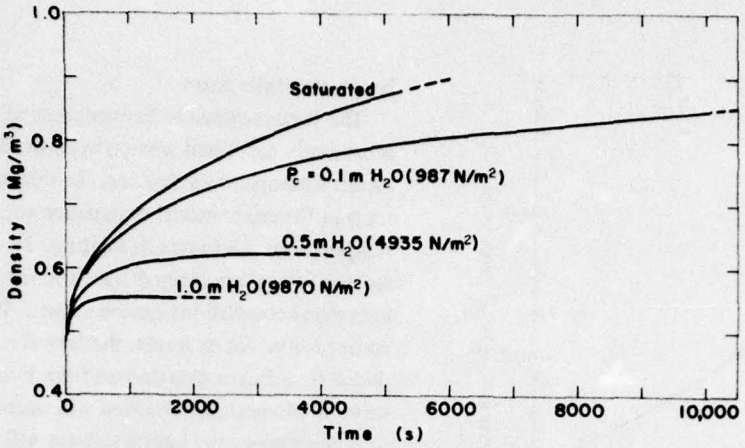

Figure 6. Calculated density shown as a function of time for four values of capillary pressure at a hydrostatic stress of 10^4 N m^{-2} and an initial particle size of 1 mm. At capillary pressures of 0.5 and 1 m H_2O, the limiting value of density is reached. These four values of capillary pressure have the same effect as would sodium chloride concentrations of 0, 4.32×10^{-4}, 2.18×10^{-3} and 4.36×10^{-3} g-moles per kg of water in saturated snow at the same stress.

Table III. The calculated deformation rates are shown for a hydrostatic stress of 10^4 N m^{-2} for four values of capillary pressure.

r_p (mm)	r_b (mm)	D (mm)	ρ (Mg m^{-3})	$P_c = 0$ $d\rho/dt$ (Mg m^{-3} s^{-1})	0.1 $d\rho/dt$ (Mg m^{-3} s^{-1})	0.5 $d\rho/dt$ (Mg m^{-3} s^{-1})	1.0 m H_2O $d\rho/dt$ (Mg m^{-3} s^{-1})
1	0	0	0.480	∞	∞	∞	∞
1+	0.164	0.136	0.5046	0.00237	0.00231	0.00210	–
1.001	0.221	0.0236	0.516	9.64×10^{-4}	9.14×10^{-4}	7.46×10^{-4}	5.36×10^{-4}
1.002	0.265	0.0338	0.532	5.64×10^{-4}	5.21×10^{-4}	3.75×10^{-4}	1.93×10^{-4}
1.005	0.336	0.0527	0.565	2.89×10^{-4}	2.53×10^{-4}	1.28×10^{-4}	–
1.01	0.400	0.0724	0.602	1.78×10^{-4}	1.45×10^{-4}	3.08×10^{-5}	–
1.02	0.475	0.0975	0.653	1.11×10^{-4}	8.00×10^{-5}	–	–
1.04	0.566	0.128	0.724	6.98×10^{-5}	3.99×10^{-5}	–	–
1.05	0.600	0.138	0.750	5.99×10^{-5}	3.03×10^{-5}	–	–
1.075	0.677	0.157	0.802	4.52×10^{-5}	1.62×10^{-5}	–	–
1.10	0.722	0.170	0.839	3.66×10^{-5}	8.19×10^{-6}	–	–
1.14	0.794	0.182	0.877	2.80×10^{-5}	7.96×10^{-7}	–	–
1.146	0.804	0.183	0.881	2.71×10^{-5}	2.24×10^{-8}	–	–

shown in Figure 5 are qualitatively very similar to the theoretical results shown in Figure 6. The rate of density increase is a decreasing function of time, and at lower water saturations, corresponding to larger capillary pressures, the maximum density asymptotically approaches a lower limit. Once this limit is reached, further compression is only possible by more efficient particle packings or intracrystalline deformation. The former is not an effective compressive mechanism at these higher densities, while the latter occurs much more slowly than the thermodynamic metamorphism described here.

The introduction of ionic impurities into the liquid phase has a dramatic effect on the mechanical properties of wet snow because the phase equilibrium temperature of the mixture is reduced. When sufficient impurities are present, the mixture temperature can be lowered beneath the inter-particle bond temperature, in which case the bonds freeze and a significant interparticle strength develops. Even if the bonds do not freeze, the heat flow away from the bonds is reduced and the rate of densification and the maximum density are reduced accordingly. Thus ionic impurities in dilute

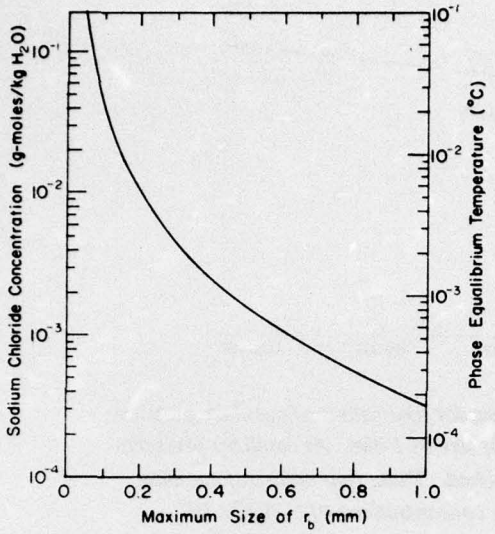

Figure 7. Maximum radius of the inter-particle bond as a function of sodium chloride concentration, shown for an initial particle size of 1 mm and a bulk stress of 2320 N m^{-2} in saturated snow. The bond size stops increasing when the pressure melting temperature of the bond surface equals the impurity temperature depression of the curved particle surface.

concentrations have the same effect on mechanical properties as capillary pressure. To illustrate this effect, the calculated curves in Figure 6 could be described as the effects of 0, 4.32×10^{-4}, 2.18×10^{-3} and 4.36×10^{-3} g-moles of sodium chloride per kg of water in saturated snow, instead of capillary pressures of 0, 987, 4935 and 9870 N m^{-2}, respectively. These levels of ionic impurities, however, are not generally found in natural snow covers away from contaminants such as road salt, while these capillary pressures are common.

The effect of impurities is clearly demonstrated in Figure 7. Like capillary pressure, ionic impurities limit the thermodynamic densification of wet snow by lowering the phase equilibrium temperature at the curved particle surface. For any given stress and initial particle size, the inter-particle bonds develop to a certain size before thermal equilibrium is reached. The limiting inter-particle bond radius r_b is shown in Figure 7 as a function of sodium chloride concentration. The rapid thermodynamic densification of wet snow is limited by the maximum size of the bond at thermal equilibrium.

Nonhydrostatic stress

The thermodynamic deformation of wet snow is most easily described when a hydrostatic bulk stress causes isotropic densification. In this case, all the contacts in the cubic model experience equal stresses, temperatures, and rates of melting. Nonhydrostatic states of stress are more difficult to interpret, but some important conclusions can be drawn. With confined compression, for example, the lateral stresses are reduced by a factor determined from Poisson's ratio, and while the largest deformation will occur along the axis of compression, the lateral stresses will give some lateral deformation. In a model where a constant sample area is maintained, a rearrangement of the particles must occur to maintain a constant cross-sectional area. The cubic model can account for this rearrangement only by allowing the discrete motion of particles to ensure a complete packing of particles in the sample area. Thus the deformation along the axis of compression would be the sum of contact melting along that axis and particle displacement from contact melting in the lateral direction. Other states of stress can be treated by similar techniques.

If one of the principal stresses is tensile, the response of wet snow can vary from immediate failure at melting bonds to considerable strength at frozen bonds. As described in the *Introduction*, the degree of freezing at the bonds is determined by parameters such as impurity content, water saturation, contact size, and history of the sample. If the bond survives the initial tensile loading, the equilibrium temperature will be raised by the tensile stress at the contact, and freezing will strengthen the contact.

CONCLUSIONS

The thermodynamics of wet snow controls its rapid deformation in a manner unlike the deformation of dry snow. Because of the presence of liquid water, wet snow can deform rapidly by melting at the inter-particle contacts and refreezing at the curved ice surfaces. The rate of deformation is controlled by the parameters which determine the temperature difference between the inter-particle contacts and the curved ice surface. The temperature of the contact is determined strictly by the force between the particles and the size of the contact. The temperature of the curved surface is determined by the particle size, ionic impurity content of the liquid

phase, and air bubble size or capillary pressure (depending on the saturation regime). As the inter-particle bond size increases, the inter-particle stress decreases and the bond temperature increases until the temperature differences around a particle are equalized. At that time rapid thermodynamic deformation ceases, and further deformation must proceed by more efficient packing arrangements and/or the normal processes of crystalline deformation.

Using a simple geometric packing arrangement and the principles of thermodynamics, a simple model of wet snow deformation has been constructed. The results of this model are qualitatively similar to the experimental results of Tusima (1973), including a lower value of maximum density at larger capillary pressures. The effect of ionic impurities on the maximum bond size has also been calculated and found to be the same as increasing the capillary pressure. The hardening effects of increasing capillary pressure and/or ionic impurity content have practical implications for strengthening snow surfaces as an aid to oversnow mobility.

LITERATURE CITED

Colbeck, S.C. (1973) Theory of metamorphism of wet snow. U.S. Army Cold Regions Research and Engineering Laboratory Research Report 313. AD 772696.

Colbeck, S.C. (1976) On the use of tensiometers in snow hydrology. *Journal of Glaciology*, vol. 17, no. 75, p. 135-140.

Harris, C.C. and N.R. Morrow (1964) Pendular moisture in packings of equal spheres. *Nature*, vol. 203, no. 4946, p. 706-708.

Kinosita, S. (1963) Compression of snow immersed in water of 0°C, I. *Low Temperature Science*, series A, vol. 21, p. 13-22.

Mellor, M. (1975) A review of basic snow mechanics. In *Snow Mechanics Symposium (Proceedings of Grindelwald Symposium, April 1974)*. International Association of Scientific Hydrology Publication no. 114, p. 251-291.

Moore, P.J. and D.V. Millar (1971) The collapse of sands upon saturation. *Proceedings of the 1st Australian-New Zealand Conference on Geomechanics*, vol. 1, p. 54-60.

Skelton, J. (1975) Interfibre forces during wetting and drying. *Science*, vol. 190, no. 4209, p. 15-20.

Tusima, K. (1973) Tests of the repeated loadings on snow. *Low Temperature Science*, series A, vol. 31, p. 57-68.

Visscher, W.M. and M. Bolsterli (1972) Random packing of equal and unequal spheres in two and three dimensions. *Nature*, vol. 239, p. 504-507.

Wakahama, G. (1968) The metamorphism of wet snow. General Assembly of Bern, *International Union of Geodesy and Geophysics, International Association of Scientific Hydrology*, p. 370-379.